Mineralogy of Yamato-791192, HED breccia and relationship between cumulate eucrites and ordinary eucrites

Kazuto Saiki[1], Hiroshi Takeda[2] and Teruaki Ishii[3]

[1] *Research Institute of Materials and Resources, Faculty of Engineering and Resource Science, Akita University, Akita 010-8502*
[2] *Research Institute, Chiba Institute of Technology, Tsudanuma 2-chome, Narashino 275-0016*
[3] *Ocean Research Institute, University of Tokyo, Minamidai 1-chome, Nakano-ku, Tokyo 164-0014*

Abstract: Cumulate eucrites and noncumulate (ordinary) eucrites are considered to have come from one (or similar) parent body and to have formed the crust of the Vesta-like asteroid. However, their relationship is not well established as to whether they have crystallized in a different magma or have differentiated within the same magma. We studied mineralogically Yamato-791192, which is a unique HED breccia with abundant cumulate eucrite and a rare ordinary eucrite clasts. The characteristics of pyroxene suggest that the polymict breccia was generated by gathering locally ordinary eucrites and cumulate eucrites. On the other hand, the Fe/Mg distribution shows that the liquid coexisting with most cumulate eucrites was too Fe-rich (mg [$=Mg/(Mg+Fe)$ atomic ratio] $=0.25-0.30$) to have crystallized as ordinary eucrites ($mg=0.35-0.40$). We also applied the liquid trapping model of fractional crystallization and calculate the change of mg of liquid and solid during fractional crystallization. This calculation suggests that if the cumulates include a large amount of residual liquid (40-50%), a cumulate eucrite ($mg=0.50-0.55$) could crystallize from ordinary eucritic liquid ($mg=0.35-0.40$). In conclusion, cumulate eucrites probably crystallized directly from slightly evolved liquid, or they are produced by fractional crystallization with a large amount of trapped liquid.

1. Introduction

Difficulty in classification of achondrites with mineralogical features intermediate between diogenites and eucrites, promoted a group of meteoriticists to use an acronym, HED (howardites, eucrites, diogenite) achondrites (Takeda *et al.*, 1983). Occurrence of such breccias can be understood by astronomical evidence linking Vesta and the HED achondrites (Binzel and Xu, 1993), and by the presence of large impact craters on Vesta observed by the Hubble Space Telescope (Thomas *et al.*, 1997). In order to clarify the problem on the formation of such breccias as an event taken place on a Vesta-like body and relationship between cumulate eucrites and ordinary eucrites, we investigated Yamato (Y)-791192 with abundant cumulate eucrite clasts and a rare ordinary eucrite clast by mineralogical techniques. The term "ordinary eucrite" has been used to designate the most common type of eucrites, which are noncumulate and equilibrated pyroxene compositions (Takeda, 1979; Nyquist *et al.*, 1986). Ordinary eucrites are ophitic or subophitic basalts, in which pigeonite is chemically homogeneous and has fine planar exsolution lamellae of augite on (001). The term "cumulate eucrite" is in-

appropriate for the Mg-rich clasts of polymict breccias, because their petrogenetic origin is unknown. The term is, however, useful to contrast cumulate eucrite with Mg-rich clast in the context of magma differentiation trend, therefore we classify the clasts by average mg ($= Mg/(Fe + Mg)$ atomic ratio) of each pyroxene grain. Diogenite (D) type has $mg > 0.63$. Binda (B) type has mg from 0.56 to 0.63. Moore County (MC) type has mg from 0.50 to 0.56. Juvinas (JV) type ($=$ordinary eucrite type) has $mg < 0.50$.

Y-791192 has been previously classified as a polymict eucrite (Yanai and Kojima, 1995), but we recently proposed that this HED achondrite may have an affinity to Type B diogenites known in the Yamato meteorite collection (Takeda *et al.*, 1998). They are also called a Y-75032-type achondrite, because Y-75032 is the largest and representative specimen. Miura and Nagao (2000) investigated noble gas isotopic compositions of Y-791192 and discussed its paring with Y-75032-type achondrites. Takeda and Mori (1985) demonstrated that Y-75032-type achondrites are link materials between diogenites and eucrites. Y-75032-type achondrites have a common characteristic texture with shocked pyroxene fragments and glassy veins and contain pyroxene fragments with chemical compositions slightly more Fe-rich than common diogenites and variable amounts of cumulate eucrite clasts. Saiki and Takeda (1999) studied pyroxene fragments of Y-791192 and Y-791439, and discussed origin of such polymict breccias. No lithic clast of ordinary eucrite has been found in the Y-75032-type breccias. Based on a possible geological setting of various types of HED breccias, postulated by Metzler *et al.* (1995), we interpreted a formation mechanism of the Y-75032-type HED breccias by a cratering event on a Vesta-like body. Many models have been proposed for the origin of eucrites, but the origin of cumulate eucrites depends on whether one accepts "Partial melting models" or "Fractional crystallization models". Ordinary eucrites and cumulate eucrites are usually discussed separately.

The "Partial melting models" are represented by Stolper (1977), who first carried out melting experiments on eucrites. He suggested that the eucritic melt is a primary magma from partial melting of a source region consisting of olivine, pyroxene, plagioclase, chromite and metallic iron. Cumulate eucrites and diogenites, as well as variations among ordinary eucrites, were explained by variations in the degrees of partial melting and the subsequent fractional crystallization.

Bartels and Grove (1991) further discussed the origin of cumulate eucrites. They conducted melting experiments at 1 bar and 1 kbar and concluded that diogenites can form by fractional crystallization of magnesian eucrite parent compositions which originated as partial melts at depth within a parent body. Cumulate eucrites, however, are likely produced from such parent magmas by fractionation in plutonic environments distinct from ordinary eucrites, resulting in the production of very iron-rich ($mg = 0.20$) residual liquids. Their model reproduces the composition of cumulate eucrites, but the iron-rich residual liquids have not been found in meteorite collections. Hewins and Newsom (1988) pointed out that the Ol-Px phase boundary in the SiO_2-Ol-An system can shift toward the Ol side as pressure becomes sufficiently high, and will then change from a reaction boundary to a cotectic line. They suggested that even a maximum fractionation process could generate the eucritic magma on the Ol-Px-An peritectic point with a 'small' pressure drop of 1 kb, rather than the equilibrium process in the Stolper's model. Cumulate eucrites are not mentioned in this model.

Fractional crystallization models attempt to explain the production of eucritic melt by fractional crystallization.   The cumulate eucrites are assumed to have crystallized after diogenites.   The fractional crystallization model was revived by Ikeda and Takeda (1985), who pointed out that the olivine-pyroxene reaction boundary will shift toward the pyroxene-anorthite join for a liquid more magnesian than the composition used by Stolper (1977), and the eucritic melt will solidify soon after the peritectic point. Longhi and Pan (1988) did a computer simulation of fractional and equilibrium crystallization.   They constructed equations for phase boundaries as functions of Mg/Fe ratio and pressure from experimental data from melting experiments on low-alkali basaltic compositions.   The simulation results indicated that fractional crystallization at 2 kbar could produce eucritic liquid.   However, 2 kbar is too high for a pressure of a parent body less than 250 km in radius.   Again in this model, there is no explanation for the origin of cumulate eucrites.

Ikeda and Takeda (1985) studied details of lithic clasts and mineral fragments in an Antarctic howardite, Y-7308.   They proposed a model for the evolutionary processes of a magma ocean on the parent body, where primary magma in the ocean was produced under reducing conditions by partial or batch melting of carbonaceous or LL chondritic material.   Fractional·crystallization of the primary magma took place in a more or less open system.   The fractionation process was introduced to explain the continuum of chemical composition of minerals in lithic clasts and fragments.   This model is the first model explaining all components of howardites, but many hypothetical steps are introduced.   For example, Na-richer magma is introduced as the source of cumulate eucrites than Na-poor eucritic magmas.

Hsu and Crozaz (1997) and Pun *et al.* (1997) have used their SIMS data of minerals on cumulate eucrites to discuss in detail the nature of the cumulate eucrite parent melts.   Recently, trapped liquid model has been positively applied to explain the origin of cumulate eucrite.   Treiman (1997) and Barrat *et al.* (2000) suggested that, if noncumulate and cumulate eucrites are indeed genetically related, the latter must contain a fraction of trapped melt.   Since these authors base their model mainly on trace element contents, we examined the model in terms of pyroxene chemistries.   In this paper we tried to clarify relationship between ordinary eucrites and cumulate eucrites by performing calculation of trapped liquid model reproducing the chemical compositions of Y-791192 pyroxenes.   In this context we further discuss the formation of the HED parent body crust, especially the origin of cumulate eucrites.

2.   Samples and experimental techniques

Polished thin sections (PTS), Y-791192,91-3 and 91-2, supplied by the National Institute of Polar Research (NIPR) were used for this study.   The PTS (,91-3) was studied by an optical microscope, and the chemical compositions of the minerals were obtained by electron probe microanalyzer (EPMA) JEOL 733 at Ocean Research Inst. (ORI) of Univ. of Tokyo, with 15 kV accelerating voltage and 12 nA sample current. The bulk compositions of exsolved pyroxene crystals were obtained by averaging individual concentrations of oxides obtained by the line analyses of $2-10 \mu m$ interval perpendicular to the exsolved lamellae.   The data were compared with those of other Y-

75032-type pyroxenes (Yanai and Kojima, 1995; Takeda *et al.*, 1998; Takeda and Mori, 1985).

Distribution of minerals with certain Mg/Fe and Na/Ca ratios were obtained using the Chemical Map Analysis (CMA) technique of the JEOL 8900 electron probe microanalyzer (EPMA) at the Ocean Res. Inst. of Univ. of Tokyo, with 15 kV accelerating voltage and 50 nA sample current. Elemental distribution maps of Al, Mg, Ca, Cr and Fe were obtained by the wave-length dispersive spectrometers and of Si, P and Na with the energy dispersive spectrometer. The maps are composed of 900×650 pixels with 10μm pixel size and 50 ms counting time. The elemental distribution maps of the same elements for the eucritic lithic clast were obtained with 500×1000 pixels of 4μm size and 50 ms counting time. The pyroxene types of diogenites and cumulate eucrites of fragments in the matrix were determined by CMA.

3. Results

3.1. Mineralogy of Y-791192

Small angular to subangular fragments less than 1 mm in diameter, of pyroxene and minor plagioclase, are set in dark glassy matrix. Sizes of the fragments are fairly uniform except for one large eucritic lithic clast (Fig. 1). The largest pyroxene fragment is 0.8×0.9 mm in size and that of plagioclase 0.3×0.6 mm. One brown eucritic pyroxene fragment (0.3×0.45 mm) shows fine exsolution lamellae. A few subrounded plagioclase crystals are 0.25×0.18 mm in size. The large eucritic clast 2.5 $\times 1.2$ mm in size is larger than that found in the PTS ,91-2 studied previously (Saiki and Takeda, 1999) and shows a variolitic texture of acicular, brown pyroxene (up to 0.1×0.6 mm) and white plagioclase (up to 0.1×0.8 mm) aligned parallel to the pyroxene crystals. A small fragment of this type measures 0.55×0.45 mm in size. This meteorite is different from major Y-75032-type achondrites, but are similar to Y-791439 that contains more ordinary eucritic (*ca.* 10 vol%) and less diogenitic components (less than 5 vol%) as in Y-75032. Y-791439 contains abundant fragments of cumulate eucrites with a fragment of ordinary eucrite pyroxene, but no lithic clast of ordinary eucrite was found in Y-791439.

Chemical compositions of pyroxene in Y-791192 (Table 1 and Fig. 2) distribute in the same regions as those of the Y-75032-type achondrites, but the diogenitic components are small and ordinary eucrite pyroxenes are more abundant than those of previously described members (Fig. 2). Saiki and Takeda (1999) recognized six types of pyroxenes in another PTS (,91-2). They are designated as D1, D2 (diogenitic), B (Binda-type), MC1, MC2 (Moore County-type), and JV (Juvinas-type ordinary eucrite). This PTS (,91-2) contains fragments of MC-type cumulate eucrite. Our PTS (,91-3) contains more Y-75032-type diogenitic pyroxenes, for example, D163, B161, B170 (Table 1). One rare fragment of MC-type in PTS (,91-3) has augite (MC 166 in Table 1) occupying a half of the grain, because of the possible oblique cut of the PTS surface to a thick augite lamella. M151 is intermediate between MC-type and B-type. The JV-type fragment (JV103) is more Mg-rich than the pigeonite in the ordinary eucrite clast (Table 1). The compositions of plagioclase fragments in the matrix show characteristics of the Y-75032 plagioclase with some high Na-rich compo-
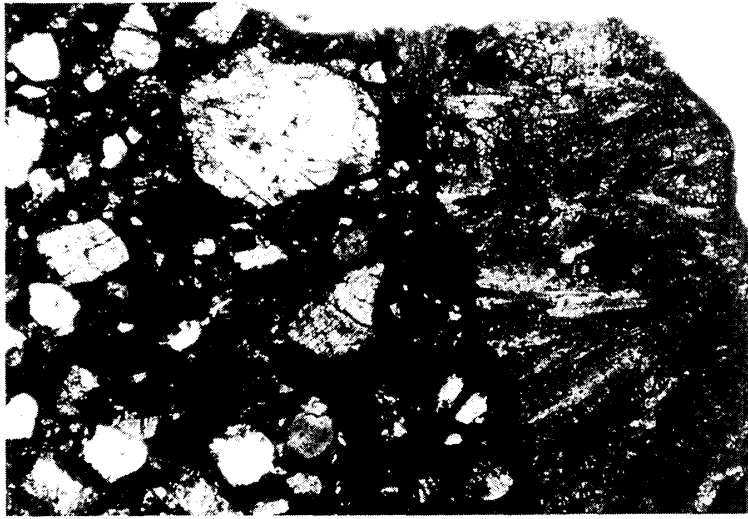
(a) General view with light colored fragments set in the dark glassy matrix. Fragments are mostly from diogenites and cumulate eucrites. A eucritic clast is located at the right side. Width is 3.3 mm.
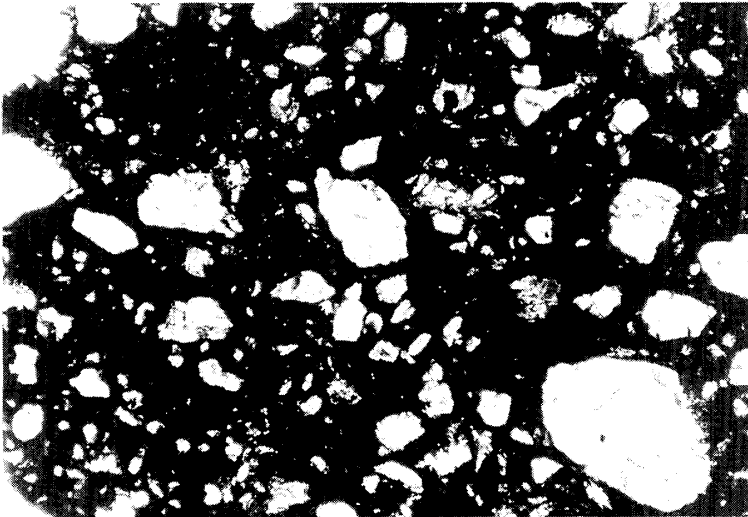
(b) Cumulate eucrite and diogenitic fragments in the matrix. Width is 1.3 mm.
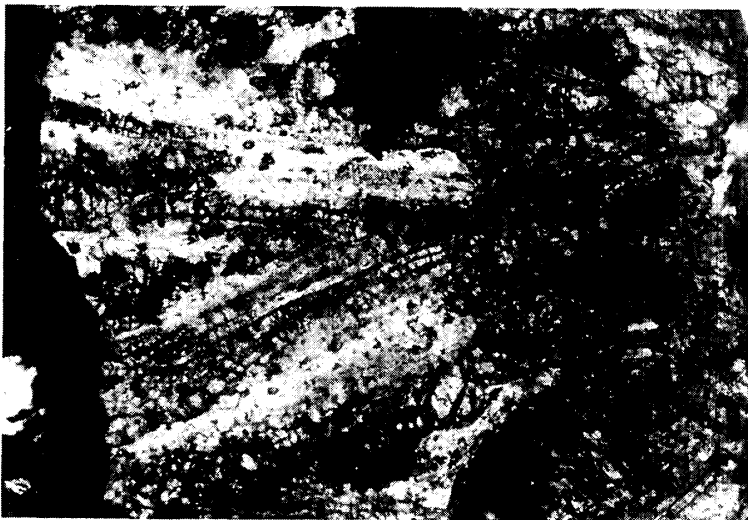
(c) A large eucritic lithic clast with variolitic texture of acicular pigeonites and plagioclase laths. Width is 1.3 mm.

Figs. 1 a–d.   Photomicrographs of Y-791192,91-3.

(d) Elemental distribution map of Y-791192,91-3. Its color indicates Mg concentration
(Red: Mg-rich, blue: Mg-poor).

sitions (Fig. 3). The glass compositions are the same as those of the Y-75032-type (Table 1).

The acicular (slightly variolitic) pyroxene crystals in the lithic clast of ordinary eucrite (JV-type) show uniform mg# with variations along the tie line of the exsolved pair (Fig. 2) in spite of its quickly grown texture. The apparently uniform compositions of the host pyroxene imply that they are equilibrated pyroxenes as were found in the type 5 pyroxene of ordinary eucrites (Takeda and Graham, 1991). The widths of the augite lamellae are in the order of a few microns. As were found in typical ordinary eucrites, the plagioclase crystals preserve chemical zoning within the crystal produced by the initial crystallization (Fig. 3). Average compositions of a lath of plagioclase at the center of the radiating texture (Fig. 1c) and the middle part do not differ significantly.

3.2. Comparison with other Y-75032-type HED achondrites

Seventeen Y-75032-type achondrites have been described in Catalog of the Antarctic Meteorites (Yanai and Kojima, 1995) with their pyroxene quadrilaterals. They showed more diversity of pyroxene chemistry than those we studied previously (Takeda and Mori, 1985; Takeda et al., 1998). To understand where we should place Y-791192 in the mineralogical variety of the Y-75032-type achondrites, we examined the pyroxene

Table 1.   *Chemical compositions (wt%) of major minerals in an ordinary eucrite clast and pyroxene fragments in the matrix of Y-791192,91-3.*

| Mineral | Eucritic Clast | | Glass | Pyroxene Fragments | | | | | | |
| | Plagioclase | | Pig.* | Pyroxene | | | | | | Pig.* |
No.	bulk EPL1	bulk EPL9	bulk EPX8	Ave. GL26	bulk D163	bulk B161	bulk B170	bulk M151	host MH166	lamella ML166	Ave. JV103
SiO$_2$	47.9	48.1	50.2	48.4	53.2	53.0	53.4	53.2	52.3	53.2	51.8
TiO$_2$	0.01	0.02	0.11	0.43	0.28	0.30	0.37	0.36	0.28	0.37	0.31
Al$_2$O$_3$	32.2	32.9	0.20	19.9	0.47	0.46	0.57	0.52	0.34	0.64	0.35
FeO	0.91	0.41	32.9	11.6	22.5	23.4	21.4	19.1	26.3	10.2	27.3
MnO	0.02	0.01	1.00	0.35	0.79	0.80	0.75	0.68	0.92	0.39	0.89
MgO	0.32	0.03	12.5	5.49	21.8	19.9	21.5	18.2	18.7	13.6	17.6
CaO	17.0	17.1	2.38	11.9	1.06	2.52	2.20	8.37	0.90	21.7	1.82
Na$_2$O	1.70	1.71	0.03	0.72	0.01	0.02	0.02	0.04	0.01	0.08	0.01
K$_2$O	0.08	0.09	0.01	0.08	0.01	0.02	0.01	0.01	0.01	0.02	0.01
Cr$_2$O$_3$	0.02	0.01	0.11	0.34	0.24	0.21	0.30	0.24	0.16	0.32	0.15
V$_2$O$_3$	0.01	0.01	0.01	0.00	0.01	0.01	0.01	0.01	0.00	0.02	0.01
Total	100.2	100.4	99.4	99.2	100.4	100.6	100.5	100.7	99.9	100.6	100.3
Fs			56.5		35.8	37.7	34.3	30.7	43.2	16.3	44.9
En			38.3		62.0	57.1	61.2	52.1	54.9	39.0	51.3
Wo			5.2		2.2	5.2	4.5	17.2	1.9	44.7	3.8
An	84.2	84.3									
Ab	15.3	15.2									
Or	0.5	0.5									

*Pig.: pigeonite; bulk: bulk compositions of minerals obtained by averaging measurements of line analysis.

mineralogy of other Y-75032-type achondrites and try to classify them into three subclasses as summarized below:

(a)   Diogenitic members

Pyroxene compositions of Y-75032, Y-791000, Y-791072, Y-791187, Y-791188, Y-791189, Y-791199, Y-791202, Y-791204, Y-791422, Y-791466, Y-791467, and Y-791603 are nearly uniform and cluster around $mg\# = Mg \times 100/(Mg + Fe)$ 67 mole% (Yanai and Kojima, 1995; Takeda *et al.*, 1998; Takeda and Mori, 1985). Y-75032-type pyroxene has $mg\#$ less than 70. Since Y-791194 and Y-791203 contains pyroxenes with compositions around $mg\# = 70$, they should belong to common diogenite group (Yanai and Kojima, 1995). Y-791188 pyroxenes include rare compositions close to $mg\# = 60$.

The crystalline portion is more abundant in hand specimen and two thin sections of Y-791199. Brecciated areas are small and form veins filling the interstices of the two crystalline clasts of pyroxene. Vein matrix contains plagioclase (*An* 90 to 82) and chromite grains (up to 0.3 mm in diameter). The pyroxene compositions cluster around Ca$_{2.5}$Mg$_{64.5}$Fe$_{33.0}$. One crystalline clast (5.8 $\times$ 3.3 mm in size) consists of coarse-grained pyroxene (up to 3 mm) with thin blebby curtain-like inclusions of augite aligned along the *c* direction. Three small triangular plagioclase grains (*An* 74 to 81) are
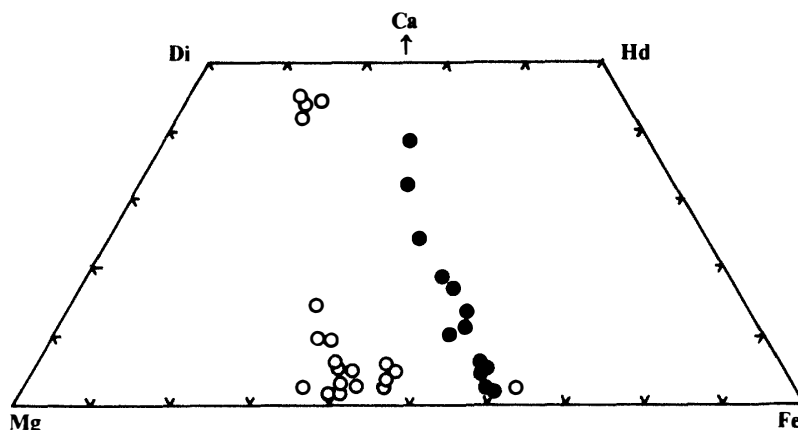
Fig. 2. Pyroxene quadrilateral of Y-791192,91-3. Solid circles: Eucritic clast; open circles: pyroxene fragments in the matrix, mostly cumulate eucrites.
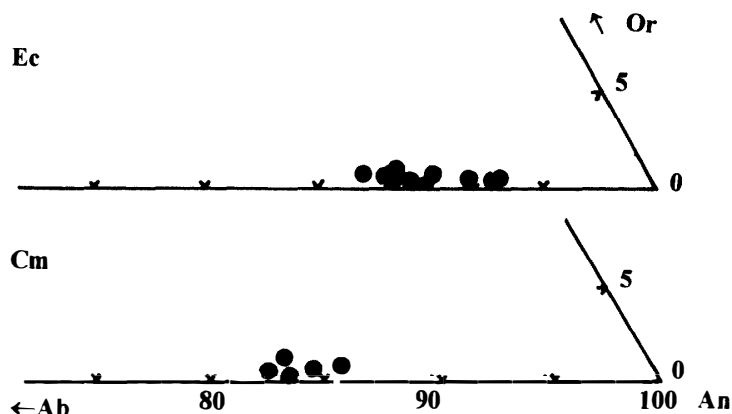

Fig. 3. Plagioclase compositions plotted in parts of the Or-Ab-An diagram. Ec: Eucritic clast; Cm: fragments in the matrix.

present at the interstices of grain boundaries of pyroxene. A diogenitic clast (5.4×1.5 mm) contains possible primary orthopyroxene with fine regular lamellae on (100) and fine chromite inclusions. The bulk chemical composition of the pyroxene is more Ca-poor and Fe-poor than that of the clast with blebby pyroxene. Almost entire PTS of Y-791422 is one crystalline clast (5×8 mm). The pyroxene composition is uniform and low in Ca ($Ca_2Mg_{67}Fe_{31}$), indicative of orthopyroxene.

Y-791000 and Y-791466 are more fragment-rich rocks, texturally similar to Y-75032. Dark brown glassy materials are penetrated into fractures of pyroxene fragments and matrices. The chemistries of pyroxene are also similar to those in Y-75032. The bulk pyroxene composition of some pyroxenes in Y-791000 with blebby augite precipitation is higher in Ca ($Ca_5Mg_{64}Fe_{31}$) than that of primary orthopyroxene. Y-791466 contains minor shocked plagioclase grains. An values of plagioclase range from 68 to 94, but chemistries of pyroxenes are fairly constant as those in Y-75032.

(b) Diogenites with cumulate eucrites

Y-791073 (Takeda, 1986), Y-791200, and Y-791201 contain pyroxenes with $mg\#$ down to 50. Y-791201 is high in cumulate eucrite abundance and low in diogenitic

component. The mg#s of pyroxene range from 70 to 50 and cover the entire range between Fe-rich diogenites and cumulate eucrites. *An* contents of plagioclase range from 86 to 93. It is not a howardite because neither basalt nor olivine is present. Some lithic clasts are composed of pyroxene, plagioclase, and minor chromite and troilite, but some rocks composed of only pyroxene are present. Devitrified, shocked plagioclase fragments are more abundant (25 vol%) than those in other Y-75032-type achondrites. The Al_2O_3 contents in the shocked glass of Y-791200 range from 5–7 wt%. Chemical compositions of shock melt glasses in Y-791201 are high in Al_2O_3 (14 wt%) and in modal plagioclase (46 vol%).

One large noritic clast (4.1 × 1.5 mm in size) attached to Y-791201, and texturally similar to the Moama cumulate eucrite, consists of orthopyroxene (36%), plagioclase (61%, An_{89}), and blebby augite (3%). Round pyroxene grains ($Ca_7Mg_{58}Fe_{35}$) about 1 mm in diameter with blebby inclusions of augite aligned along one crystallographic direction may be low-Ca inverted pigeonite. The bulk pyroxene composition is intermediate in mg# between the pyroxene fragments in the matrix. Plagioclase is shocked, but only a part of the crystal is maskelynite.

(c) Cumulate eucrites with diogenites and rare eucrites

This group includes the sample of this study and Y-791439. Y-791439 contains eucritic pyroxenes, but no lithic clast has been found. Y-791439 contains more abundant clasts of cumulate eucrite than those of Y-75032. We observed six clasts (to 2.8 × 2.3 mm) in the PTS. Saiki and Takeda (1999) divided pyroxene chemical compositions of Y-791439 into four types: diogenite-type, Binda-type, Moore County-type, and rare Juvinas-type. The diogenite-type pyroxenes are the most magnesian in the meteorite, and are similar to Fe-rich diogenites. The Binda-type pyroxenes are the most abundant, and many of them preserve the original lithic clast shape. The chemical compositions of Binda-type pyroxenes are slightly more Fe-rich than Binda, but many of them have blebs typical of the Binda cumulate eucrite. The chemical compositions of other two types are close to those of Moore County and those of Juvinas. Minor plagioclase grains are present in the matrix.

3.3. Estimation of magma chemistry

We calculated the mg of equilibrium liquid coexisting with the pyroxenes (Fig. 4) in Y-791439 and Y-791192 from their mg numbers using the equation: "[Fe/Mg]$_{pyroxene}$ = [Fe/Mg]$_{liquid}$ * KD". KD is a solid-liquid distribution coefficient between pyroxene and liquid. We use a KD of 0.30 (Stolper, 1977; Grove, 1978; Longhi and Pan, 1988; Barrat *et al.*, 2000). We explain the data in Fig. 4 using Y-791192 as an example. The liquid equilibrated with the pyx92(D1) pyroxene (mg = 0.68) corresponds to bulk compositions of ordinary eucrites (mg = 0.39). There is a possibility that the pyx92(D1) pyroxenes crystallized from the liquid which would solidify as an ordinary eucrite such as pyx92(JV) because the mg of pyx92(JV) (mg = 0.41) and the mg of equilibrium liquid (mg = 0.39) with pyx92(D1) are almost the same. The liquids equilibrated with Fe-rich pyroxenes (pyx92(B+MC)) are more evolved magmas than ordinary eucrite's bulk composition. For Y-791439, the same argument can be made. Most D-type pyroxenes could be cumulus from the liquid which has the same mg of JV-type pyroxenes. The equilibrated liquid coexisting with most MC and B-type pyroxenes are
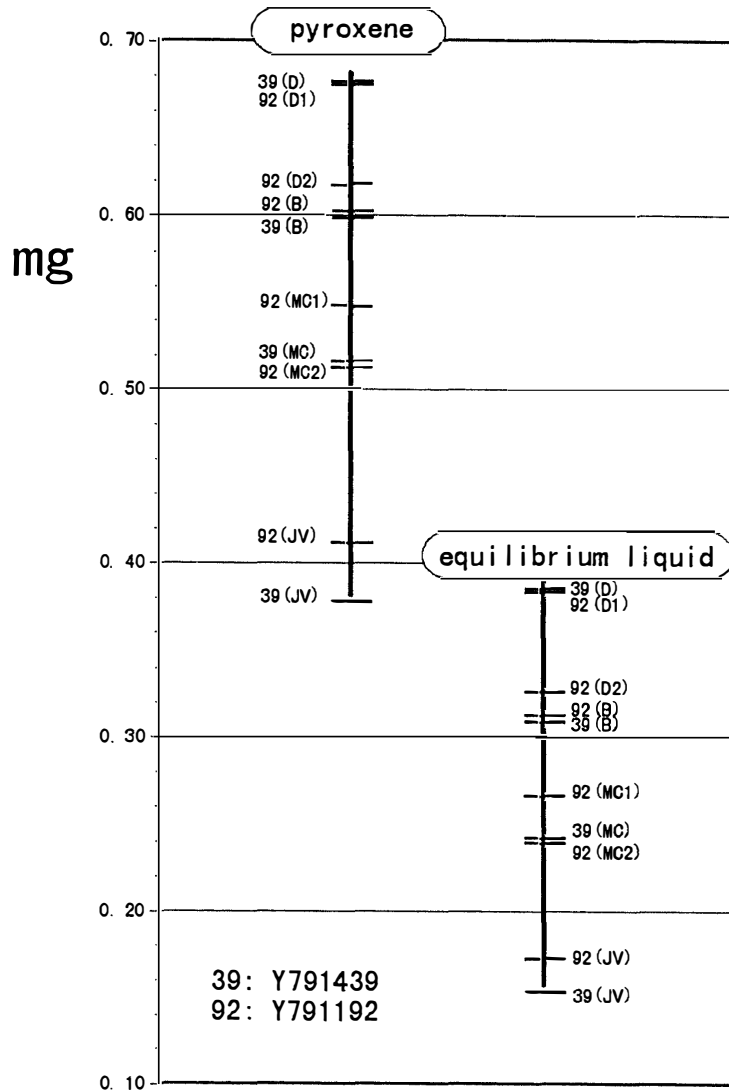
Fig. 4. Chart showing mg of pyroxenes of eucrites and their coexisting liquids. The chemical compositions of Y-791439, Y-791192, are obtained in this study. The left column shows observed chemical compositions and the right column shows calculated equilibrium liquid compositions.

too Fe-rich to be ordinary eucrite.

To examine the efficiency of the trapped liquid hypothesis, the "mg"s of liquid and instantaneous solid (IS) crystallized by a fractional crystallization process with/without trapped liquid were calculated. The source program list for this calculation is presented as appendix. Fractional crystallization with trapped liquid can be simulated with very simple program. The program prepares hypothetical liquid composed only of FeO and MgO. (In other words, we can detect only FeO and MgO within the magma and the other componennts are invisible.) It calculates IS composition using the Fe/Mg distribution coefficient between pyroxene and liquid and fractionates a hypothetical pyroxene composed of MgO and FeO with 0.1 vol% of the initial volume. This calculation is repeated until the volume fraction reaches 99 vol%. We use oxygen units

to estimate the volume fraction. Supposing that all crystals and melt have a volume similar to close packing of oxygens, the number of oxygen is a good indicator of volume fraction. For the calculation, the distribution coefficient between pyroxene and liquid (KD = 0.30) is used (Stolper, 1977; Grove, 1978; Longhi and Pan, 1988; Barrat *et al.*, 2000). In the early stage olivine also crystallizes. KD for olivine is about 0.35, but small amount of olivine do not have a severe affect on the result. The Y-7308 howardite bulk composition (Ikeda and Takeda, 1985) is a candidate for the bulk crust compositions of the HED parent body because it contains both surface rock and cumulate rock from the deepest crust or upper mantle (diogenites) among known howardites; therefore, its initial *mg* (= 0.7) is used. If the ratio of pyroxene and plagioclase during crystallization does not change drastically, and if large amounts of minor mafic phases (chromite, ilmenite, Fe-metal etc.) do not crystallize, this calculation is a good analog of magma in fractional crystallization.
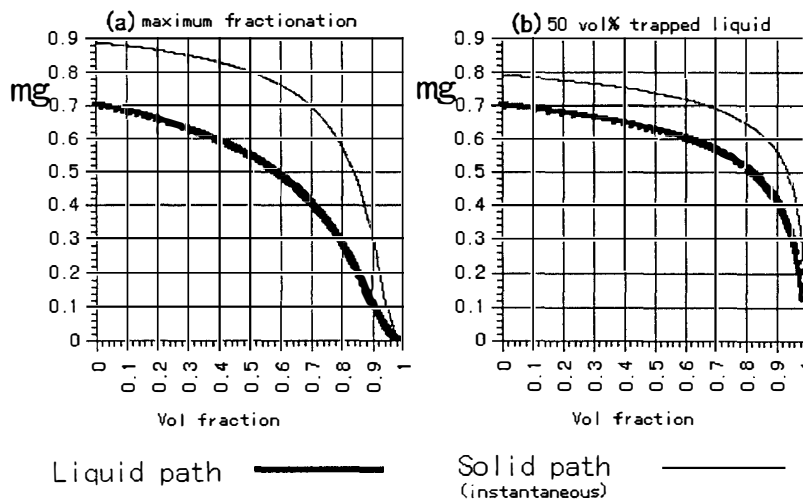

Fig. 5.   The liquid path and instantaneous solid path in fractional crystallization.
(a) The case of maximum fractional crystallization.
(b) The case of fractional crystallization with variable amount of trapped liquid.
   The calculation assumes trapped liquid of 50% volume fraction in cumulus.

Calculation of the maximum fractionation of mafic elements is shown in Fig. 5a. The process, in which crystals were completely separated from liquid. When the *mg* of fractionated pyroxene reaches the *mg* of Fe-rich cumulate eucrite (*ex. mg* = 0.55), over 18 vol% liquid remains. The remnant liquid has *mg* = 0.27. This liquid is too Fe-rich to become ordinary eucrite. The results of fractional crystallization with 50% trapped liquid are shown in Fig. 5b. In this case, Fe-rich cumulate eucrite can be produced without hypothetical Fe-rich liquid. When the amount of trapped liquid is around 50 %, Fe-rich cumulate eucrite(*ex. mg* = 0.55) could be produced from ordinary eucritic liquid (*mg* = 0.40) and the volume of this remnant liquid is *ca.* 9%. This liquid can be solidified as ordinary eucrite.

4. Discussion

4.1. Classification of Y-791192 and related achondrites

Y-791192 has been classified as a polymict breccia, but this study supports its reclassification as an unusual howardite or polymict cumulate eucrite with affinity to Y-75032 (Yanai and Kojima, 1995). Mittlefehldt and Lindstrom (1993) noticed that large pyroxene clasts in Y-791192 are compositionally similar to those of the Y-75032 -type achondrites, but did not find varieties of cumulate eucrites characteristics of this specimen. Saiki and Takeda (1999) divided pyroxene chemical compositions of Y-791439 into six types. We examined all pyroxene fragments in the PTS by chemical mapping techniques, and corelated chemistry with their exsolution and inversion textures (Fig. 1d). The diogenite-type pyroxenes are similar to Fe-rich diogenites. The chemical compositions of Binda-type pyroxenes are slightly more Fe-rich than Binda, but many of them have blebs typical of the Binda cumulate eucrite. Minor plagioclase grains are present in the matrix.

The pyroxene fragments of the JV-type of Y-791192 are similar to those of Y-791439 ($Ca_{15}Mg_{35}Fe_{50}$), but Y-791192 contains an ordinary eucrite clast with variolitic texture. The eucritic clast shows dark fine-grained variolitic texture of brown pyroxene and white lathes of plagioclase, but their pyroxenes are homogenized. This observation implies that the metamorphic event took place before this breccia formation event.

The pairing of Y-75032-type achondrites are mostly based on their unique shock melt veins and clustered pyroxene compositions around $mg\#$ 67 together with exsolution and inversion textures. Other members with abundant cumulate eucrites share the above common features with the diogenite-rich members. Since it is difficult to identify fragments of diogenitic pyroxene from the Binda-type pyroxene in cumulate eucrites, we can classify Y-791192 as an unusual howardite. Mittlefehldt and Lindstrom (1993) pointed out that Y-791192 should be reclassified as a howardite. However, they did not recognize that some of the Y-75032-type pyroxene are the Binda-type inverted pigeonite. The definition of diogenite implied that pyroxene should be primary orthopyroxene. Since the amounts of ordinary eucrite and diogenitic orthopyroxene are small ($< 10\%$), Y-791192 can be a polymict cumulate eucrite.

Another key item, which links these meteorites as a paired sample, is the presence of pyroxene with thin blebby, wavy, augite inclusions aligned along one orientation. Their bulk compositions (e.g., $Ca_5Mg_{64}Fe_{31}$ of Y-791000) are lower in mg numbers than those in cumulate eucrites like Binda (e.g., $Ca_7Mg_{58}Fe_{35}$ of Y-791201), but is higher than those of primary orthopyroxene (e.g., $Ca_2Mg_{67}Fe_{31}$ of Y-791422). The exsolution mechanism of these pyroxenes has been explained in our previous work (Takeda and Mori, 1985). The Binda-type pyroxene is a product of decomposition of pigeonite at the Pigeonite-Eutectoid-Reaction (PER) line (Ishii and Takeda, 1974). Because the bulk composition of the Y-791000 pyroxene lies between primary orthopyroxene and one at the PER line, the low-Ca clinopyroxene crystal will go through the orthopyroxene-pigeonite inversion loop upon cooling from crystallization temperature. When the cooling is slow, orthopyroxene lamellae will be produced in the clinopyroxene with (100) in common. This lamella will grow thicker as temperature goes down. If the bulk composition of the crystal is close to the PER line, the clinopyroxene crystal

will still remain, when it reaches at the PER line.   Then, it will decompose into augite and orthopyroxene.   This product may have thinner augite blebs than those of the Binda-type pigeonite, because of the low initial bulk Ca contents.   Because this kind of pyroxene can be produced only for a special low-Ca chemistry and cooling rates (Ishii and Takeda, 1974), the presence of such pyroxene can be used as a key to identify the pairing and deduce cooling history.

Combined textural and chemical studies of Y-75032-type pyroxene revealed that these achondrites experienced shock event in the history of the crustal evolution before they finally ejected from the Vesta-like body by the last large impact as was observed as large craters by Hubble Space Telescope on Asteroid 4 Vesta (Thomas *et al.*, 1997). The presence of ordinary eucrite clast in Y-791439 and Y-791192 suggests that the excavation took place after the global crustal metamorphism as suggested by Yamaguchi *et al.* (1996).   The preservation of partly maskelynitized plagioclase and impact melt glass implies that thermal annealing did not take place after the last impact event.

4.2.   Magma differentiation trend of the HED parent body

Because varieties of cumulate eucrites have been found in Y-791192, it is appropriate to examine how such cumulate eucrites can be produced by magma differentiation. Our calculation of equilibrium liquid coexisting with cumulate eucrites showed that a large amount of Fe-rich liquid ($mg < 0.3$) is necessary to make cumulate eucrite by maximum fractionation.   Sometimes small highly Fe-rich clasts are found in the polymict breccias, *e.g.*, fayalite-silica clasts reported in Y-7308 (Ikeda and Takeda, 1985).   However, there is not enough Fe-rich liquid to buffer the mg number during fractionation of cumulate eucrites.

Considering the fact that even in terrestrial gravity, 25–50 vol% inter-cumulus liquid can remain (Anthony, 1990), it is natural to think that cumulate eucrite has a large amount of inter-cumulus liquid.   However, after the liquid has solidified as an over-growth of cumulus crystals, and then recrystallized by annealing, it is very difficult to identify whether or not there initially existed inter-cumulus phase.   We tested this proposed trapped liquid model for the origin of cumulate eucrites with our computer program.   If the cumulus includes large amount of residual liquid (50%), cumulate eucrite ($mg = 0.55$) (Fig. 5b) could crystallize from ordinary eucritic liquid ($mg = 0.40$).   If there were variable amounts of trapped liquid, many kinds of cumulate eucrites could be produced.

The calculation results also indicate that slightly evolved liquid itself could have cumulate eucrite composition.   Some cumulate eucrites, especially Fe-rich ones (*e.g.*, Y-791195) may not be cumulus but slightly evolved liquid itself slowly solidified underneath a thick ordinary eucrite proto-crust, or a strongly recrystallized upper crust. If such cumulate-eucritic liquid should exist, part of the liquid would flow over the proto-crust and solidify as a Mg-rich lava-like eucrite.   Y-791438 has Mg-rich bulk pyroxene compositions ($Ca_8Mg_{5\bullet}Fe_{42}$) similar to Nagaria and Medanitos (Symes and Hutchison, 1970; Hutchison *et al.*, 1977; Kiesl *et al.*, 1978), and has the quickly cooled texture of ordinary eucrite (Saiki *et al.*, 1991).   It may be a candidate for a Mg-rich liquid which came up near the surface.   However, there is no other eucrite that has both Mg-rich compositions and texture like ordinary eucrite.   The Y-791195-like texture

(Takeda, 1991) can be produced by thermal metamorphism by the heat of hot magma beneath it. Such early crystallized crust had a higher chance of extensive thermal metamorphism by the heat from a residual magma ocean beneath the thin crust.

With our renewed interest in the cumulate eucrites, two individual specimens in this study and another Mg-rich eucrite (Y-791195) are interpreted in terms of magma differentiation. Based on its major element chemistries and non-preferred orientation texture, we suggested that Y-791195 (Takeda, 1991) is a good candidate for evolved liquid itself. It may be an Mg-rich noncumulate eucrite. The REE pattern of Y-791195, however, shows that it is similar to cumulate eucrites in its bulk chemistry, and is intermediate between Serra de Magé and Moore County in the REE contents (Mittlefehldt and Lindstrom, 1993). In view of the trapped liquid model, the presence of Fe-rich cumulate eucrite is acceptable, but its low REE contents cannot be explained at present. It is, however, more natural to assume the presence of low REE source than high-Fe magma, because the REE concentrations can be adjusted during the partial melting processes which produced source magma. Testing our model based on the REE chemistry is another big issue to be conducted in a future work.

4.3. Geological setting of the ancient HED crust

We can postulate the following image for the ancient HED crust on the basis of the above study. In the early stage, the surface of the HED parent body was widely melted. Then, fractional crystallization occurred from the surface of magma with a large amount of trapped liquid. After a while, the surface was covered with thin proto-crust that had ordinary eucritic compositions and the interior below the proto-crust was half liquid with a slightly less Mg rich composition than JV and half solid with diogenitic compositions. At depth of the magma, diogenite layer had been formed by fractionation without appreciable trapped liquid. Below the proto-crust, fractional crystallization proceeded and according to the ratio of trapped liquid, series of cumulate eucrites are formed. Some cumulate eucrites were formed by solidification of slightly evolved liquid itself below the proto-crust. In the course of fractionation, there were many impact events which produced the quickly cooled pyroxenes and introduced heterogeneity into the formation of crust.

Metzler et al. (1995) postulated a possible geological setting of various types of HED breccias. They considered a crater formation on the possible structure of the HED parent body crust with the rock sequence basalts-gabbro-pyroxenite with increasing depth after Takeda (1979, 1982, 1997). Then, they constructed a diagram, which represents a cross section through an impact crater that modified the primary rock sequence and let to the formation of various kinds of breccias, dikes and shock veins. However, this issue has been discussed by Eugster and Michel (1995), who showed that peaks in cosmic-ray exposure ages of HED meteorites contain essentially all types, showing that a single impact event launched diogenites, eucrites, cumulate eucrites, polymict eucrites and howardites. For example, the 21 Ma age group includes Shalka, Y-75032, Binda, Sioux County, Petersburg, and Bununu essentially the entire suite of HED meteorites. The origin of the Y-75032-type breccias should take into account the fact that they were not formed by deposition of impact ejecta or fall out. Such deposits may include all components of a layered crust as in howardites and polymict eucrites

(Takeda, 1982, 1997). Close association of Fe-rich diogenites and cumulate eucrites with rare ordinary eucrites suggests that formation mechanism of these breccias are different from that of normal howardite, which might have been formed by one of the large impacts at the crater floor of Vesta (Thomas *et al.*, 1997). If we accept a picture of an impact crater of Metzler *et al.* (1995), the Y-75032-type breccias might be formed by one impact event proposed by Eugster and Michel (1995), but near the crater floor where the boundaries of diogenites and cumulate eucrites were disturbed by impact and mixed with impact melts and rare eucritic fragments in local scale.

5. Conclusions

Among many models proposed to explain the origin of eucrites, none of them can explain the variation of eucrites, especially cumulate eucrites, without adding a hypothetical liquid. In this work, two polymict breccias have been investigated to check the systematic variation of pyroxenes' composition. All kinds of pyroxenes in the PTS are observed and classified. To investigate the differentiation path of the HED magma, the *mg* of equilibrium liquid coexisting with pyroxenes in polymict breccia were calculated. To test our "liquid trapping model", we calculated the fractional crystallization of mafic elements. *Mg* number of liquid and instantaneous solid (IS) in the fractional crystallization process were calculated. The results are summarized as follows:

(1)   Characteristic textures with impact melt glass and pyroxene textures and chemistry suggest that Y-791192 is rather similar to Y-791439 and belongs to a subclass of the 75032-type HED achondrites, which contains more eucritic component.

(2)   The existence of mixtures of ordinary and cumulate eucrites in polymict breccias Y-791439 and Y-791192 indicates that the polymict breccia was generated by gathering locally ordinary eucrite and several kinds of cumulate eucrites on the HED parent body.

(3)   Formation of such complex breccias can be best explained by a geological setting with a cratering event proposed for the layered crust model of the Vesta-like body (Takeda, 1997).

(4)   The *mg* numbers of liquids coexisting with pyroxenes from cumulate eucrite clasts of Y-791192 and Y-791439 show that the liquid coexisting with most cumulate eucrites is too Fe-rich. Cumulate eucrites used to be regarded as cumulus from evolved Fe-rich liquid. However, there is no such Fe-rich clast in HED meteorites except for rare fayalite-silica clasts (Ikeda and Takeda, 1985). Small amounts of Fe-rich magma could not buffer the *mg* number during fractionation of cumulate eucrites. If we assume that cumulate eucrites are the residue of partial melt, the liquid produced from the cumulate eucrites is too Fe-rich for eucrite.

(5)   We proposed the trapped liquid model for the origin of cumulate eucrites and tested this model with our computer program. If the cumulus includes large amount of residual liquid (50%), cumulate eucrite (*mg* = 0.50–0.55) could crystallize from ordinary eucritic liquid (*mg* = 0.35–0.40). If there were variable amounts of trapped liquid, many kinds of cumulate eucrites could be produced. There is a possibility that the set of pyroxenes in the polymict breccias were produced by a single fractional crystallization

path with trapped liquid.

Acknowledgments

References

Anthony, R.P. (1990): Principles of Igneous and Metamorphic Petrology. Prentice Hall.

Bartels, K.S. and Grove, T.L. (1991): High-pressure experiments on magnesian eucrite compositions; constraints on magmatic processes in the eucrite parent body. Proc Lunar Planet. Sci. Conf., **21**, 351–365.

Barrat, J.A., Blichert-Toft, J., Gillet, Ph. and Keller, F. (2000): The differentiation of eucrites: The role of in situ crystallization. Meteorit. Planet. Sci., **35**, 1087–1100.

Binzel, R.P. and Xu, S. (1993): Chips off of asteroid 4 Vesta: Evidence for the parent body of basaltic achondrite meteorites. Science, **260**, 186-191.

Eugster, O. and Michel, Th. (1995): Common asteroid break-up events of eucrites, diogenites, and howardites and cosmic-ray production rates for noble gases in achondrites. Geochim. Cosmochim. Acta, **59**, 177–199.

Grove, T.L. (1978): Experimentally determined FeO-MgO-CaO partitioning between pyroxene and liquid in lunar basalts (abstract). EOS, **59**, 401.

Hewins, R.H. and Newsom, H.E. (1988): Igneous activity in the early solar system. Meteorites and the Early Solar System, ed. J.F. Kerridge and M.S. Matthews. Tucson, University of Arizona Press, 73–101.

Hsu, W. and Crozaz, G. (1997): Mineral chemistry and the petrogenesis of eucrites: 2. Cumulate eucrites. Geochim. Cosmochim. Acta, **61**, 1293–1302.

Hutchison, R., Bevan, A.W.R. and Hall, J.M. (1977): Appendix to the Catalogue of Meteorites: with Special Reference to Those Represented in the Collection of the British Museum (Natural History). London, British Museum (Natural History), 297 p.

Ikeda, Y. and Takeda, H. (1985): A model for the origin of basaltic achondrites based on the Yamato 7308 howardite. Proc. Lunar Planet. Sci. Conf., 15th, Pt. 2, C649-C663 (J. Geophys. Res., **90** Suppl.)

Ishii, T. and Takeda, H. (1974): Inversion, decomposition and exsolution phenomena of terrestrial and extraterrestrial pigeonites. Mem. Geol. Soc. Jpn., **11**, 19–36.

Kiesl, W., Weinke, H.H. and Wichtl, M. (1978): The Medanitos meteorite. Meteoritics, **31**, 513–516.

Longhi, J. and Pan, V. (1988): Phase equilibrium constraints on the howardite-eucrite-diogenite association. Proc. Lunar Planet. Sci. Conf., 18th, 459–470.

Metzler, K., Bobe, K.D., Palme, H., Spettel, B. and Stoffler, D. (1995): Thermal and impact metamorphism of the HED parent body. Planet. Space Sci., **43**, 499–525.

Mittlefehldt, D.W. and Lindstrom, M.M. (1993): Geochemistry and petrology of a suite of the Yamato HED meteorites. Proc. NIPR Symp. Antarct. Meteorites, **6**, 268–292.

Miura, Y.N. and Nagao, K. (2000): Noble gases in Y-791192, Y-75032-type diogenites, and A-881838. Antarctic Meteorites XXV, Tokyo, Natl Inst. Polar Res., 85–87.

Nyquist, L.E., Takeda, H., Bansal, B.M., Shih, C.Y., Wiesmann, H. and Wooden, J.L. (1986): Rb-Sr and Sm-Nd internal isochron ages of a subophitic basalt clast and a matrix sample from the Y75011

eucrites.   J. Geophys. Res., **91**, 8137–8150.

Pun, A., Papike, J. J. and Layne, G.D. (1997): Subsolidus REE partitioning between pyroxene and plagioclase in cumulates: An ion microprobe investigation.   Geochim. Cosmochim. Acta, **61**, 5089–5097.

Saiki, K. and Takeda, H. (1999): Origin of polymict breccias on asteroids deduced form their pyroxene fragments.   Meteorit. Planet. Sci., **34**, 271–283.

Saiki, K., Takeda, H. and Tagai, T. (1991): Zircon in magnesian, basaltic eucrite Yamato 791438 and its possible origin.   Proc Lunar Planet. Sci., **21**, 341–349.

Symes, R.F. and Hutchison, R. (1970): Medanitos and Putinga, two South American meteorites.   Mineral. Mag., **37**, 721.

Stolper, E. (1977): Experimental petrology of eucritic meteorites.   Geochim. Cosmochim. Acta, **41**, 587–611.

Takeda, H. (1979): A layered crust model of a howardite parent body.   Icarus, **40**, 445–470.

Takeda, H. (1982): Mineralogical characteristics of polymict breccias on the howardite parent body and the moon.   LPI Tech. Rep., **82-02**, 148–150.

Takeda, H. (1986): Mineralogy of Yamato 791073 with reference to crystal fractionation of the howardite parent body.   Proc. Lunar Planet. Sci. Conf., 16th, Pt. 2, D355–D363 (J. Geophys. Res., **91**, B4).

Takeda, H. (1991): Comparisons of Antarctic and non-Antarctic achondrites and possible origin of the differences.   Geochim. Cosmochim. Acta, **55**, 35–47.

Takeda, H. (1997): Mineralogical records of early planetary processes on the howardite, eucrite, diogenite parent body with reference to Vesta.   Meteorit. Planet. Sci., **32**, 841–853.

Takeda, H. and Graham, A.L. (1991): Degree of equilibration of eucritic pyroxenes and thermal metamorphism of the earliest planetary crust.   Meteoritics, **26**, 129–134.

Takeda, H. and Mori, H. (1985): The diogenite-eucrite links and the crystallization history of a crust of their parent body.   Proc. Lunar Planet. Sci. Conf., 15th, Pt. 2, C636–C648 (J. Geophys. Res., **90** Suppl.)

Takeda, H., Mori, H., Delaney, J.S., Prinz, M., Harlow, G.E. and Ishii, T. (1983): Mineralogical comparison of Antarctic and non-Antarctic HED (howardites -eucrites-diogenites) achondrites.   Mem. Natl Inst. Polar Res., Spec. Issue, **30**, 181–205.

Takeda, H., Saiki, K. and Ishii, T (1998): Yamato diogenite-cumulate-eucrite breccias: their classification and formation on a Vesta-like body.   Antarctic Meteorites XXII, Tokyo, Natl Inst. Polar Res., 148–150.

Thomas, P.C., Binzel, R.P., Gaffey, M.J., Storrs, A.D., Wells, E.N. and Zellner, B.H. (1997): Impact excavation on Asteroid 4 Vesta: Hubble Space Telescope results.   Science, **277**, 1492–1495.

Treiman, A.H. (1997) The parent magmas of the cumulate eucrites: A mass balance approach.   Meteorit. Planet. Sci., **32**, 217–230.

Yamaguchi, A., Taylor, G.J. and Keil, K. (1996): Global crustal metamorphis of the eucrite parent body.   Icarus, **124**, 97–112.

Yanai, K. and Kojima, H. (1995): Catalog of the Antarctic Meteorites. Tokyo, Natl Inst. Polar Res., 230 p.

Appendix

For examining the efficiency of trapped liquid, we wrote a small program for fractional crystallization of mafic mineral with/without trapped liquid.   The source list of this program is shown below.   This program is written in C language.

```
/***************************************** list start *****************************/

#include <stdio.h>

#include <math.h>

void main()

{

        FILE  *fp.*fopen();

        double liq_mg;              /* mg of total liquid */

        double sol_mg;              /* mg of instantaneous solid */


        double kd = 0.30;         /* Fe/Mg distribution coefficient (Stolper, 1977) */

        double step = 0.001;        /* fractionation step (now 0.1 vol%) */

        double ratio;          /* volume ratio of trapped liquid */

        double f;                   /* degree of fractionation (vol amount of solid) */


        fp = fopen("result.dat"."w");

        printf("\nMg/(Mg+Fe) of initial liquid ? (0-1.0): ");

        scanf("%lf".&liq_mg);

        printf("\nRatio of trapped liquid ?     (0-1.0):");

        scanf("%lf".&ratio);


        for(f=0;f<0.99;f=f+step){

                sol_mg = 1/((1/liq_mg-1)*kd+1);     /* mg of equilibrium solid */

                sol_mg = ratio * liq_mg + (1-ratio) * sol_mg;    /* mg of solid to be removed */

                if(f!=0)

                        liq_mg = ((1-f+step)*liq_mg - step * sol_mg) / (1-f);  /* fractionation */

                fprintf(fp."\n%5.3f\t%5.3f\t%5.3f".f.liq_mg.sol_mg);

                }

        fprintf(fp."\n");

        fclose(fp);

        printf("\nEnd");

}

/*************************** list end *****************************************/
```

When you execute this program, it requests the *mg* of initial liquid and the ratio of trapped liquid.   Input them with your keyboard.   If you want to calculate the *mg* path in maximum fractionation, assign 0 as the ratio of trapped liquid.   Then the output file "result.dat" is created in the current directory.   The format of this output file is as follows.

```
/*************************** list start ****************************************/

0.000   0.700        0.889

0.001   0.700        0.889

0.002   0 700        0.889

            :      :

/************************** list end *******************************************/
```

Data is separated by TAB and lines are separated by CR/LF.   The first column shows the volume solid fraction.   The second shows the *mg* of liquid and the third shows the *mg* of instantaneous solid (including trapped liquid).   You can import the output file into a spreadsheet application and make the same kind of graph as Fig. 5.